Supplementary Material

for

Electron Transport through Thin Organic Films in Metal-Insulator-Metal Junctions Based on Self-Assembled Monolayers

R. Erik Holmlin,[1] Rainer Haag,[1] Michael L. Chabinyc,[1] Rustem F. Ismagilov,[1] Adam E. Cohen,[1] Maria Anita Rampi,[2,*] Andreas Terfort,[1] and George M. Whitesides[1,*]

Note: All references to equations and figure that are not preceded by 'S' refer to the main text.

Experimental Results

Parametric Sensitivity of the Data: We tested the sensitivity of the current-voltage (I-V) measurements of the $J_{Ag\text{-}SAM(1)//C_{16}\text{-}Hg}$ junctions to a variety of preparatory conditions. We outline the details of these studies in the following sections.

Roughness of the Film: Figure S1 compares I-V curves for $J_{Ag\text{-}C_{10}//C_{16}\text{-}Hg}$ junctions in which the Ag film was either 100 or 200 nm thick. The data from both thicknesses are nearly identical within experimental error.

Area of Contact: Figure S2 shows the dependence of the current (at a bias = 0.5 V) flowing across $J_{Ag\text{-}C_{10}//C_{16}\text{-}Hg}$ as a function of the area of contact between the two SAMs; Figure S2B shows the current density calculated for each datum in Figure S2A. To determine the area

of contact, we used a video camera to visualize the area of contact and magnify it by a factor of 100; we then measured the diameter of the magnified area of contact (relative to a standard) on a video screen using a micrometer. The uncertainty of the measurement of the diameter on the video screen was ~ ± 1-2 mm; this uncertainty corresponds to an error of ~5 x 10^{-4} cm^2, or ~35%, in the actual contact area. This observation suggests that uncertainty in the area of contact is a significant determinant of the uncertainty

Solvent: We examined the dependence of the I-V curves for a number of organic solvents (Fig. S3). We examined isooctane because it should not be able to intercalate within the thiols that make up the films on the electrodes. Hexane was selected as an example of an organic solvent comparable to hexadecane and toluene was selected as an example of an aromatic solvent. THF and acetonitrile were selected as examples of polar organic solvents with heteroatoms. The data from the polar solvents were less informative. The current density of the junction formed in freshly distilled THF that had been degassed with argon could not be differentiated from the background current of several nA that was observed with the SAM-coated electrodes in close proximity but not in contact. With acetonitrile, the junction melted—that is, the Hg electrode merged with the Ag electrode—as soon as a potential of even a few mV was placed across it. Acetonitrile does not dissolve C_{16}-SH and the presence of this thiol in solution around the junction is essential for its stability so it is not surprising that this solvent could not be tested.

Purity of Thiols and Preparation of SAMs: Figure S3 compares the current density across a junction under standard conditions to that for a junction fabricated with SAMs on Ag that had been formed by exposing a Ag film to a solution containing a mixture of C_{10}-SH (1 mM) and C_{10}-S-S-C_{10} (1 mM) in ethanol for 24 h. We also compared the current density across

junctions comprising SAMs on Ag that were formed under different conditions. SAMs on Ag incubated for ~24 h in a solution of C_{10}-SH did not perform differently than SAMs on Ag that had incubated at room temperature for 1 week. The performance of junctions comprising SAMs that were formed in solutions of thiols that had been degassed by bubbling Ar through them for ~15 min was the same as those comprising SAMs formed with aerated solvents.

Reproducibility

The standard deviations from the average current density, computed for N-1 degrees of freedom (where N = 21) and the 95% confidence intervals are shown as error bars in Fig S4B and S4C. The magnitude of the standard deviations were approximately ± 55% of the average current density for each bias voltage. The 95% confidence intervals—the range of current density within which we have 95% confidence that the real mean value is present—are shown as error bars about the average current density in Figure S4C. The confidence intervals ranged from approximately +25% to –25% of the average current density.

Modeling of I-V Data

Figure S5 shows a comparison of the experimentally determined attenuation factors, β, and those calculated using Eq. 10 for a junction with structure $J_{Ag\text{-}C_{10}//C_{16}\text{-}Hg}$. We used the parameters—barrier ϕ_0 = 0.67 V, distance d=3.9 nm, preexponential factor C_0 =3.5, and a =1—derived from Eq. 10 at a bias of 0.1V to predict the voltage dependence of β. Although the measured and calculated values of β agree at low bias, the calculated values decrease by ~50% over the range of 0.1 to 1 V; the measured values do not decrease over this range. We find better agreement with the modified parameters —barrier ϕ_0 = 2.1 V, distance d=3.9 nm,

preexponential factor C_0 =3.5, and a =0.67—derived from the nonlinear least squares fit to Eq. 9.

Confidence Intervals for the Fitted I-V Curves.

We sought to estimate confidence intervals for the calculated curves that were obtained by fitting the experimental data. These intervals define a region above and below the fitted value of current density within which the true predicted value (according to the equation used to fit the data) lies.

We calculated the standard deviation of the sample population (s) for 21 different I-V curves (Figure S4) with Equation S1, where $\bar{x}$ is the average current density, x_i is the ith value of current density, and N is the number of independent measurements; the 95% confidence intervals for average values of I at a given bias voltage (Figure S4) were calculated with Equation S2.[1]

$$s = \frac{\sqrt{\sum_i (\bar{x} - x_i)^2}}{\sqrt{N-1}} \qquad \text{(S1)}$$

$$95\%\ \text{Conf. Int.} = \bar{x} \pm 2.09\left(\frac{s}{\sqrt{N}}\right) \qquad \text{(S2)}$$

A computer program (Origin v. 6.1) was used to estimate confidence intervals for the fitted I-V curves in Figure S6. The routine involved fitting the 21 independent I-V curves (418 data) to Equation 9 with fixed values of $\alpha = 0.62$ and $\phi_0 = 2.1$; the preexponential factor (C_0) to was allowed to float. An automatic routine within the software then calculated the confidence intervals for the fitted curves. Figure S6 shows these intervals along with the experimental data and the best fit to Equation 9. Despite the fairly large range in the current density, the confidence interval is approximately ± 10% of the fitted value at each applied potential. The

width of the intervals depends strongly on the number of data used in the fitting; removing data widens the interval substantially.

References

1. Gonick, L.; Smith, W. *The Cartoon Guide to Statistics*; HarperPerennial: New York, 1993; p. 22 and p. 135.

Figure Captions

Figure S1. Plots of current density as a function of bias potential for junctions with structure $J_{Ag\text{-}C_{10}//C_{16}\text{-}Hg}$. The plot shows eight independent experiments (four with Hg biased anodically and four with Hg biased cathodically) for eight different junctions in which the thin silver film supporting the C_{10} SAM was 100 nm thick, and eight independent experiments for eight different junctions in which the silver film was 200 nm thick. The symbols are defined on the plot.

Figure S2. (A) Plot of current as a function of the area of contact between SAMs in a junction with structure $J_{Ag\text{-}C_{10}//C_{16}\text{-}Hg}$. The plot shows data for three experiments, and the average current for each area of contact. The symbols are defined on the plot. The length of the error bars were calculated by assuming an error of 0.1 cm in the diameter of contact. (B) Plot of current density for the data in (A).

Figure S3. Plot of average current density (from 0 to 1 V) for a junction with structure $J_{Ag\text{-}C_{10}//C_{16}\text{-}Hg}$ under standard conditions (solvent = hexadecane) against current density (from 0 to 1 V) for junctions with the same structure but under different conditions (solvent or preparation of SAM on Ag). The symbols are defined on the plot. The solid line represents the theoretical line expected when the current density on the y-axis is equal to that on the x-axis.

Figure S4. Plots of current density as a function of bias voltage for junctions with structure $J_{Ag-C_{10}//C_{16}-Hg}$. (A) I-V curves for 21 independent junctions (out of 30 junctions assembled). (B) Plot of the average current density as a function of bias voltage. The error bars represent standard deviations. (C) Same as (B), but the error bars represent 95% confidence intervals for the mean at each bias voltage.

Figure S5. Plots comparing the attenuation factor β determined experimentally for a junctions with structure $J_{Ag\text{-}SAM(1)//C_{16}\text{-}Hg}$, where SAM(1) on Ag was formed from aliphatic thiols (solid symbols) to the attenuation factor β calculated (solid lines) with Equation 10 in the text; the parameters used in the calculation of the different curves are indicated on the plots.

Figure S6. Confidence intervals for the curve obtained by nonlinear least squares fitting of I-V curves from 21 independent junctions to Equation 9. The intervals represent the 95% confidence level. The inset shows an expansion of the plot to emphasize the upper and lower confidence lines. The best fit to Equation 9 is the solid in between the confidence interval.

Figure Captions

Figure S1. Plots of current density as a function of bias potential for junctions with structure $J_{Ag\text{-}C_{10}//C_{16}\text{-}Hg}$. The plot shows eight independent experiments (four with Hg biased anodically and four with Hg biased cathodically) for eight different junctions in which the thin silver film supporting the C_{10} SAM was 100 nm thick, and eight independent experiments for eight different junctions in which the silver film was 200 nm thick. The symbols are defined on the plot.

Figure S2. (A) Plot of current as a function of the area of contact between SAMs in a junction with structure $J_{Ag\text{-}C_{10}//C_{16}\text{-}Hg}$. The plot shows data for three experiments, and the average current for each area of contact. The symbols are defined on the plot. The length of the error bars were calculated by assuming an error of 0.1 cm in the diameter of contact. (B) Plot of current density for the data in (A).

Figure S3. Plot of average current density (from 0 to 1 V) for a junction with structure $J_{Ag\text{-}C_{10}//C_{16}\text{-}Hg}$ under standard conditions (solvent = hexadecane) against current density (from 0 to 1 V) for junctions with the same structure but under different conditions (solvent or preparation of SAM on Ag). The symbols are defined on the plot. The solid line represents the theoretical line expected when the current density on the y-axis is equal to that on the x-axis.

Figure S4. Plots of current density as a function of bias voltage for junctions with structure $J_{Ag-C_{10}//C_{16}-Hg}$. (A) I-V curves for 21 independent junctions (out of 30 junctions assembled). (B) Plot of the average current density as a function of bias voltage. The error bars represent standard deviations. (C) Same as (B), but the error bars represent 95% confidence intervals for the mean at each bias voltage.

Figure S5. Plots comparing the attenuation factor β determined experimentally for a junctions with structure $J_{Ag\text{-}SAM(1)//C_{16}\text{-}Hg}$, where SAM(1) on Ag was formed from aliphatic thiols (solid symbols) to the attenuation factor β calculated (solid lines) with Equation 10 in the text; the parameters used in the calculation of the different curves are indicated on the plots.

Figure S6. Confidence intervals for the curve obtained by nonlinear least squares fitting of I-V curves from 21 independent junctions to Equation 9. The intervals represent the 95% confidence level. The inset shows an expansion of the plot to emphasize the upper and lower confidence lines. The best fit to Equation 9 is the solid in between the confidence interval.

Figure S1

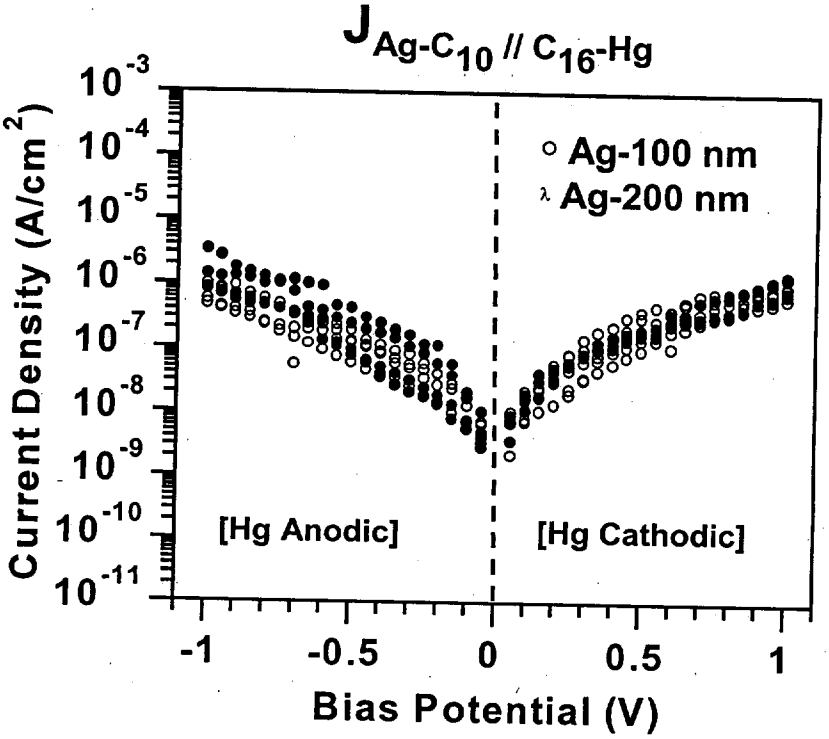
J Ag-C10 // C16-Hg
Current Density (A/cm2)
10-3
10-4
10-5
10-6
10-7
10-8
10-9
10-10
10-11
Ag-100 nm
Ag-200 nm
[Hg Anodic]
[Hg Cathodic]
-1
-0.5
0
0.5
1
Bias Potential (V)

Figure S2

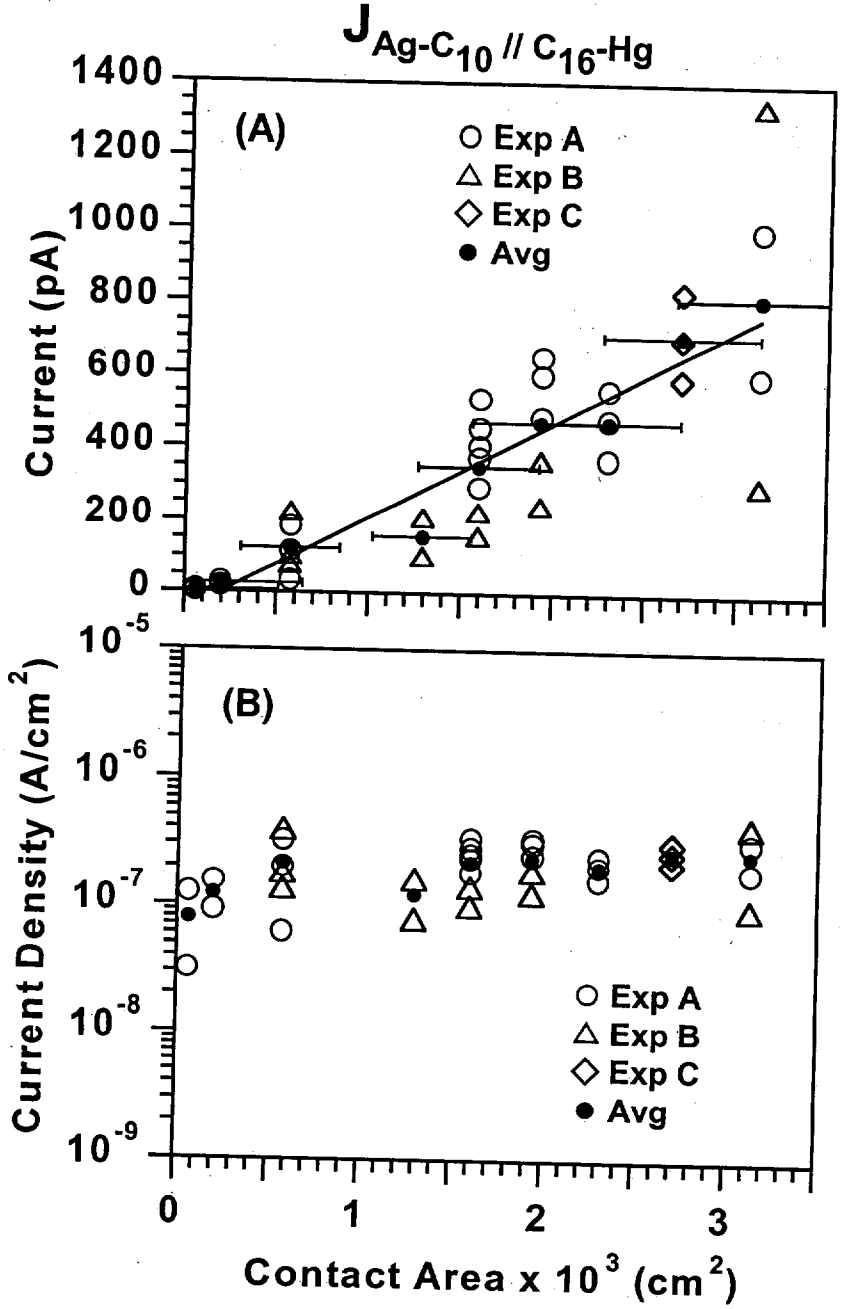

Figure S3

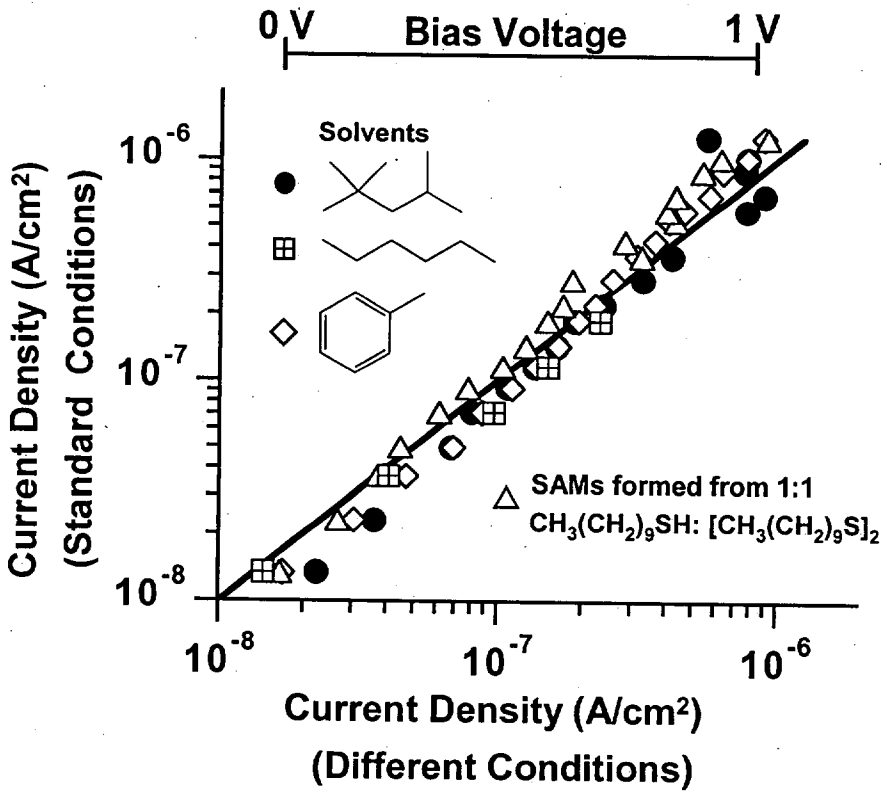

Figure S4

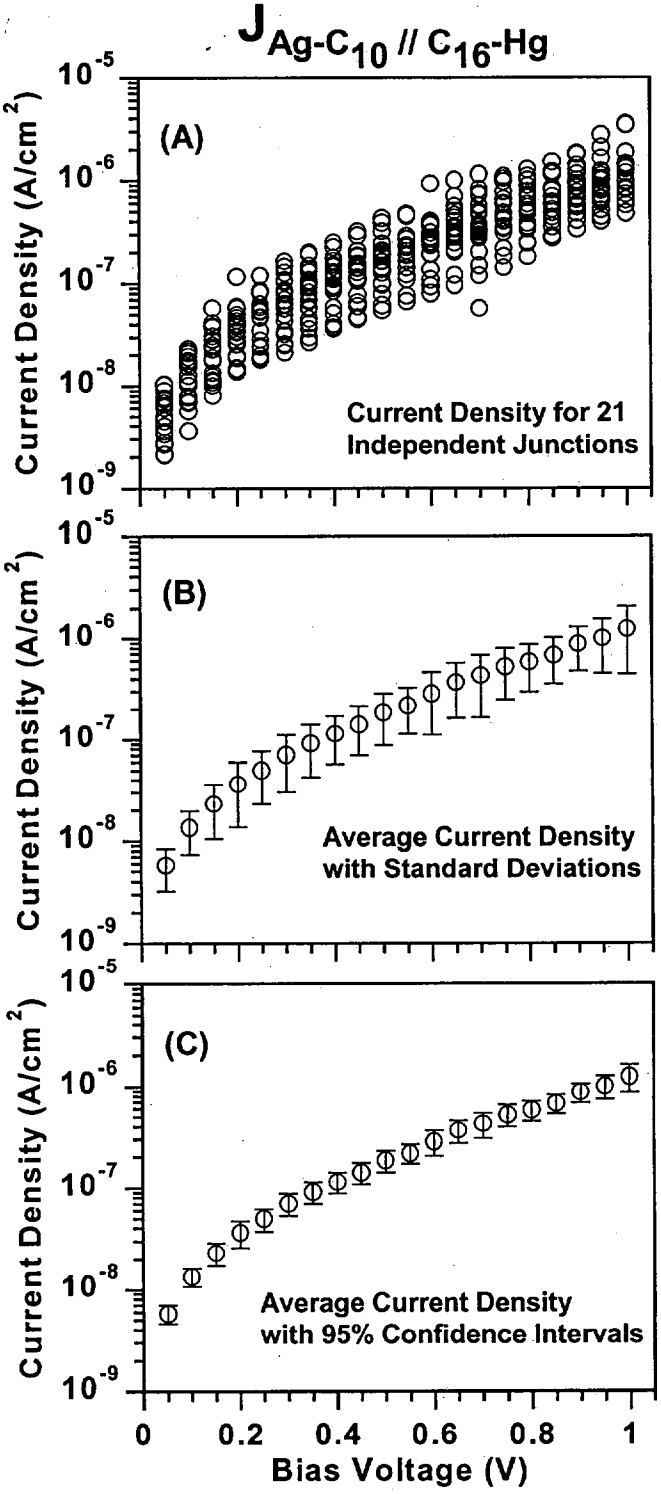

Figure S5

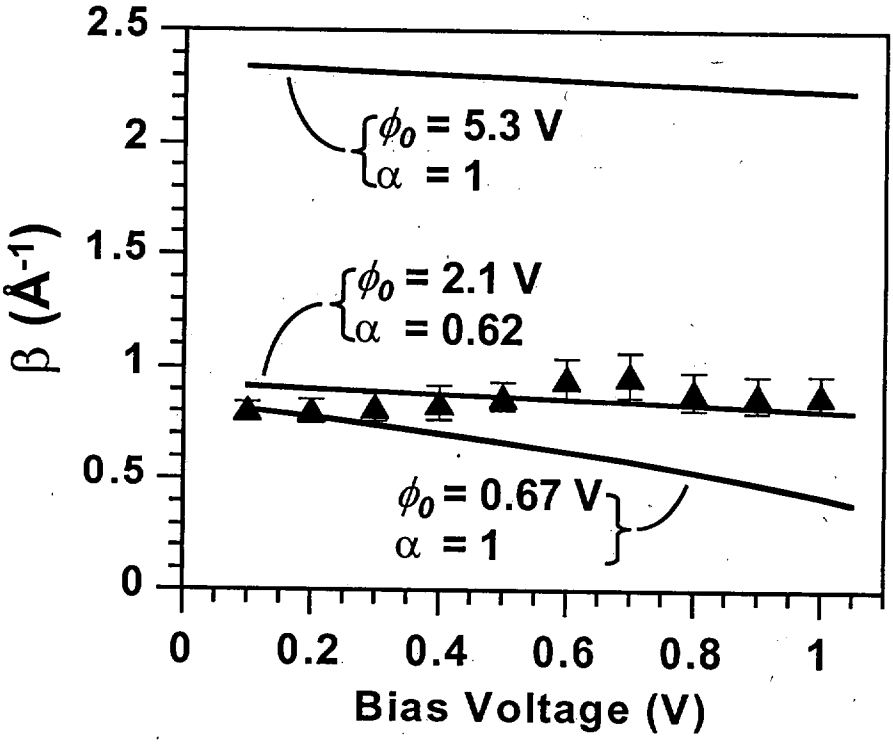

Figure S6

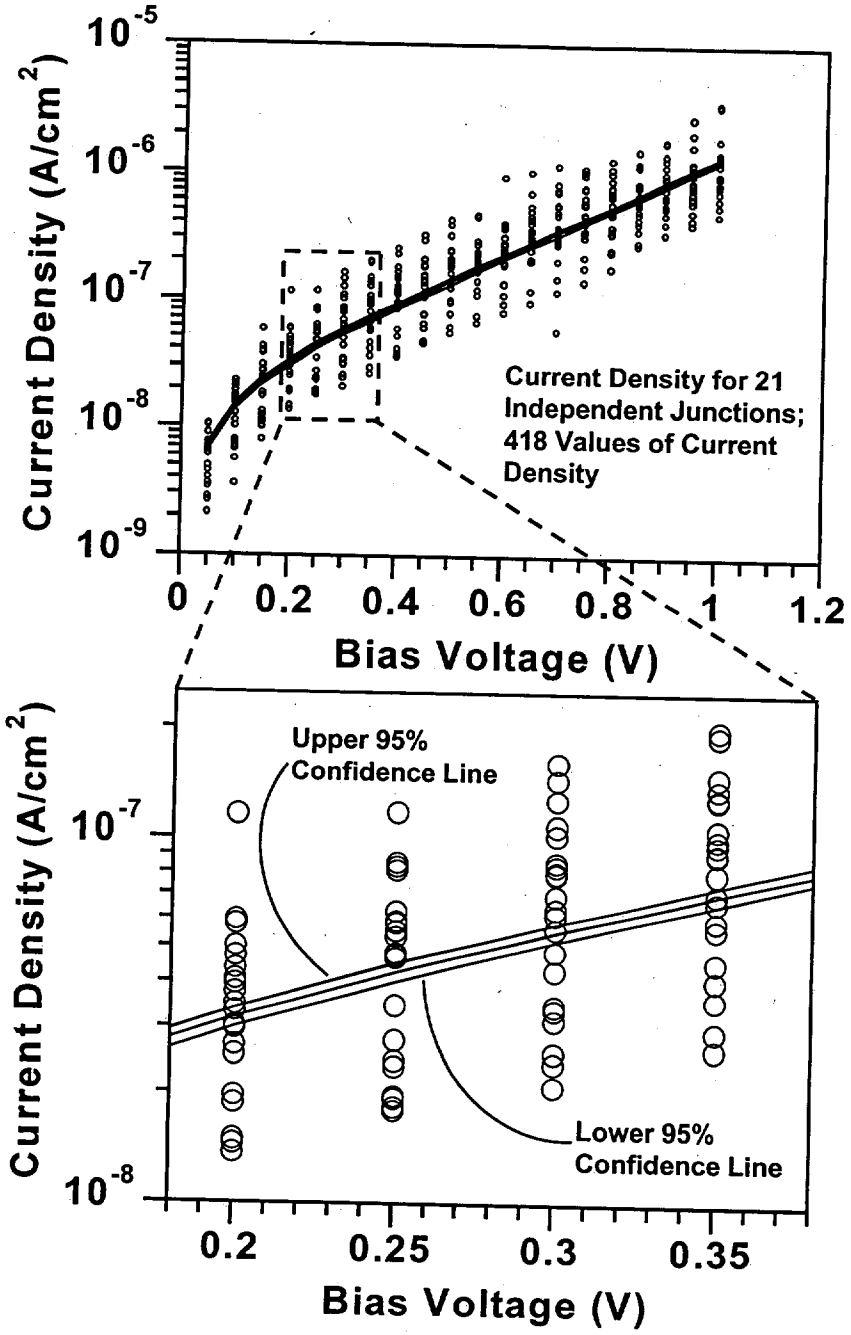
Current Density (A/cm^2)
10^{-5}
10^{-6}
10^{-7}
10^{-8}
10^{-9}
0
0.2
0.4
0.6
0.8
1
1.2
Bias Voltage (V)
Current Density for 21 Independent Junctions; 418 Values of Current Density
Current Density (A/cm^2)
10^{-7}
10^{-8}
Upper 95% Confidence Line
Lower 95% Confidence Line
0.2
0.25
0.3
0.35
Bias Voltage (V)